

# Continuously Tunable Microwave Frequency Multiplication by Optically Pumping Linearly Chirped Fiber Bragg Gratings in an Unbalanced Temporal Pulse Shaping System

Hiva Shahoei, *Student Member, IEEE*, and Jianping Yao, *Fellow, IEEE, Fellow, OSA*

**Abstract**—We propose and demonstrate a new and simple method for achieving continuously tunable microwave frequency multiplication using an unbalanced temporal pulse shaping (TPS) system incorporating two linearly chirped fiber Bragg gratings (LCFBGs) written in erbium/ytterbium co-doped fibers. By optically pumping the LCFBGs with different pumping power, the dispersion of the LCFBGs is tuned. The incorporation of the LCFBGs in an unbalanced TPS system would enable the generation of a frequency tunable microwave waveform. The operation of the system is discussed which is then verified by an experiment. Continuously tunable microwave frequency multiplication with a multiplication factor from 5.14 to 11.9 is experimentally demonstrated. The impact of the ripples in the magnitude and group delay responses of the LCFBGs on the performance of the microwave generation is also studied.

**Index Terms**—Frequency multiplication, linearly chirped fiber Bragg grating (LCFBG), real-time Fourier transform, temporal pulse shaping (TPS).

## I. INTRODUCTION

MICROWAVE signal synthesis in the optical domain is an interesting topic which can find many applications such as in radar, communications, and microwave tomography [1]–[3]. In the past few years, numerous techniques have been proposed [4]–[7]. In [4], microwave frequency division or multiplication was demonstrated through dispersively stretching or compressing a highly chirped optical pulse that is modulated by a microwave signal. The achievable maximum microwave frequency is limited by the dispersion-induced power penalty due to the use of optical double-sideband (DSB) modulation. In [5], optical single-sideband (SSB) modulation is used; the limitation in [4] is, thus, eliminated. However, the implementation of the SSB modulation requires the use of a dual-port intensity modulator and a broadband 90° hybrid, which may increase the complexity of the system. Recently, an approach

to achieving frequency multiplication based on a general temporal self-imaging effect has been proposed [6]. The frequency upshifting of the microwave signal from 10 to 50 GHz was demonstrated. The limitation of this method is that the multiplication factor can only be tuned to specific values since the focused image of the microwave drive signal can only be obtained under specific dispersion conditions called integer Talbot conditions. In [7], continuously tunable frequency multiplication was achieved by using an unbalanced temporal pulse shaping (TPS) system consisting of two dispersive elements. The tuning was demonstrated by tuning the dispersion of the dispersive elements in the system. In the experimental demonstration, a 6.1 km dispersion compensating fiber was used as the first dispersive element and a length of a single-mode fiber (SMF) as the second dispersive element. By changing the length of the second dispersive element, the tunability of the multiplication was demonstrated. The problem associated with this technique is that the length of the SMF should be changed to achieve frequency tuning which is hard to implement for fast and continuous frequency tuning. In addition, the lengths of the two fibers are long in order to have large dispersion, which makes the system bulky with poor stability.

In this paper, we propose and experimentally demonstrate an approach to achieving continuously tunable frequency multiplication using an unbalanced TPS system incorporating two linearly chirped fiber Bragg gratings (LCFBGs) written in erbium/ytterbium (Er/Yb) co-doped fibers. Compared with an LCFBG written in a regular photosensitive fiber, the dispersion of an LCFBG written in an Er/Yb co-doped fiber can be tuned by optically pumping the LCFBG [8], [9]. The incorporation of two Er/Yb co-doped LCFBGs in an unbalanced TPS system would enable the all-optical and continuous tuning of the multiplication factor. The key significance of the approach compared with the one in [7] is that the microwave frequency can be continuously tunable. In addition, the Er/Yb co-doped LCFBGs have much shorter lengths of a few centimeters, which makes the system more compact with better stability.

It is different from a typical TPS system where the two dispersive elements have complementary dispersion. Here, in the unbalanced TPS system, the Er/Yb co-doped LCFBGs are designed to have opposite dispersion, but nonidentical in magnitude. Thus, the entire system can be considered as a typical TPS system with two dispersive elements having complementary dispersion for real-time Fourier transformation (FT) [10]

Manuscript received October 04, 2011; revised February 28, 2012; accepted March 07, 2012. Date of publication April 03, 2012; date of current version April 13, 2012. This work was supported by the Natural Science and Engineering Research Council of Canada (NSERC).

The authors are with the Microwave Photonics Research Laboratory, School of Electrical Engineering and Computer Science, University of Ottawa, Ottawa, ON K1N 6N5, Canada (e-mail: jpyao@eecs.uottawa.ca).

Color versions of one or more of the figures in this paper are available online at <http://ieeexplore.ieee.org>.

Digital Object Identifier 10.1109/JLT.2012.2190581

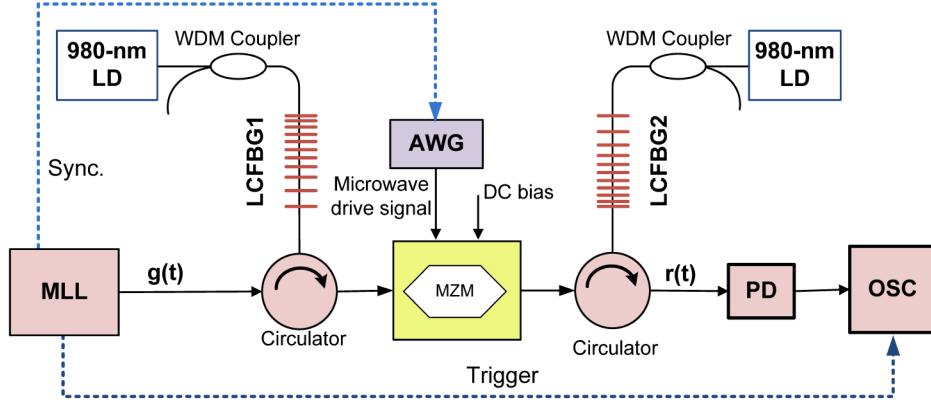


Fig. 1. Unbalanced TPS system proposed to achieve continuously tunable frequency multiplication. The LCFBGs are optically pumped to change the dispersion.

followed by a residual dispersive element to achieve a second real-time FT. The operation of the system is discussed which is then verified by an experiment. Continuously tunable microwave frequency multiplication with a multiplication factor from 5.14 to 11.9 is experimentally demonstrated. The impact of the ripples in the magnitude and group delay responses of the LCFBGs on the performance of the microwave generation is also studied.

## II. PRINCIPLE

The proposed unbalanced TPS system for microwave generation with continuously tunable frequency is shown in Fig. 1. The system consists of a mode-locked laser (MLL), two LCFBGs written in Er/Yb co-doped fibers pumped by two 980-nm laser diodes (LDs), two optical circulators, a Mach-Zehnder modulator (MZM), and a high-speed photodetector (PD). A microwave drive signal generated by an arbitrary waveform generator (AWG) is applied to the MZM. The generated microwave signal is monitored by a sampling oscilloscope.

An LCFBG can be modeled as a linear time-invariant system with a transfer function given by

$$H_i(\omega) = \exp\left(-j\frac{\ddot{\Phi}_i\omega^2}{2}\right), \quad (i = 1, 2) \quad (1)$$

where  $\ddot{\Phi}_i$  (in square picoseconds) is the dispersion of the  $i$ th LCFBG, and  $j = \sqrt{-1}$ . In the proposed unbalanced TPS system, the values of dispersion of the two LCFBGs should satisfy  $\ddot{\Phi}_1\ddot{\Phi}_2 < 0$ , and  $|\ddot{\Phi}_1| \neq |\ddot{\Phi}_2|$ . In fact, the unbalance TPS system can be seen as a typical balanced TPS system with two complementary dispersive elements followed by a third dispersive element with a residual dispersion of  $\Delta\ddot{\Phi} = \ddot{\Phi}_1 + \ddot{\Phi}_2$ . The transfer function of the residual dispersive element is given by  $H_\Delta(\omega) = \exp(-j(\Delta\ddot{\Phi}\omega^2)/(2))$ . It is known that a DSB modulated signal will experience power penalty if the signal is traveling in a dispersive element. To eliminate the dispersion-induced power penalty [4], in our proposed system, the MZM is dc-biased at the minimum transmission point to suppress the optical carrier. Under the small-signal-modulation condition, the intensity modulation function of the MZM can

be written as  $e_{\text{IM}}(t) = 2 \times J_1(\beta) \cos(\omega_m t)$ , where  $J_1(\beta)$  is the first-order Bessel function of the first kind,  $\beta$  is the phase modulation index, and  $\omega_m$  is the angular frequency of the microwave drive signal applied to the MZM [7], [11]. If the complementary dispersion in the typical TPS system is large enough, i.e.,  $\ddot{\Phi}_1 \gg \tau_0^2$ , where  $\tau_0$  is the pulse width of the input optical pulse  $g(t)$  to LCFBG1, the signal at the output of the typical TPS system is given by [12]

$$s(t) \propto g(t) * E_{\text{IM}}(\omega)|_{\omega=2\pi t/\ddot{\Phi}_1} = J_1(\beta)[g(t - T_1) + g(t + T_1)] \quad (2)$$

where  $E_{\text{IM}}(\omega)$  is the Fourier transform of  $e_{\text{IM}}(t)$ ,  $*$  denotes the convolution operation, and  $T_1 = \omega_m \ddot{\Phi}_1 / 2\pi$ . Based on (2), it can be seen that two time-delayed replicas of the input pulse are generated at the output of the typical TPS system. By propagating the signal  $s(t)$  through the residual dispersive element, a frequency multiplied microwave signal is generated. Assume that the dispersion of the residual dispersive element satisfies the condition given by  $\Delta\ddot{\Phi} \geq T_1^2/2$ ; then, the signal at the output of the residual dispersive element is a Fourier-transformed version of  $s(t)$ , which is given by [10]

$$r(t) \approx \exp\left[\frac{jt^2}{(2\Delta\ddot{\Phi})}\right] S(\omega)|_{\omega=2\pi t/\Delta\ddot{\Phi}} = \exp\left[\frac{jt^2}{(2\Delta\ddot{\Phi})}\right] J_1(\beta) G\left(2\pi\frac{1}{\Delta\ddot{\Phi}}t\right) \cos\left(2\pi\frac{T_1}{\Delta\ddot{\Phi}}t\right) \quad (3)$$

where  $G(\omega)$  is the Fourier transform of the input pulse  $g(t)$ . The signal at the output of the PD is

$$I(t) = Rr(t)^2 = K \exp\left(-\frac{t^2}{\tau^2}\right) \left[1 + \cos\left(2\pi\frac{2T_1}{\Delta\ddot{\Phi}}t\right)\right] \quad (4)$$

where  $R$  is the responsivity of the PD,  $K = RJ_1^2(\beta)\pi\tau_0^2/2$  is a time-independent constant, and  $\tau = \sqrt{2\Delta\ddot{\Phi}}/\tau_0$  is the output pulse width. As can be seen from (4), a microwave signal with a frequency of  $\omega_{\text{RF}} = 2\pi|(2T_1)/(\Delta\ddot{\Phi})| = \omega_m((2\ddot{\Phi}_1)/(\Delta\ddot{\Phi}))$  is generated at the output of the unbalanced TPS system. Thus, the frequency multiplication factor of the proposed system is

$$F = \frac{\omega_{\text{RF}}}{\omega_m} = 2 \left(\frac{\ddot{\Phi}_1}{\Delta\ddot{\Phi}}\right). \quad (5)$$

From (5), we can conclude that frequency multiplication factor of the system is determined by the dispersion of the first LCFBG  $\ddot{\Phi}_1$  and the residual dispersion  $\Delta\ddot{\Phi}$ .

By optically pumping an LCFBG that is written in an Er/Yb co-doped fiber, the refractive index of the fiber would change [8]. Mathematically, the change of the refractive index as a function of the power change along the fiber is given by

$$\Delta n = \frac{\partial n}{\partial T} \times \frac{-\eta}{2\pi bh} \times \frac{dP_P(z)}{dz} \quad (6)$$

where  $n$  is the refractive index and  $T$  is the temperature,  $(\partial n)/(\partial T)$  is the index temperature coefficient,  $b$  is the outer radius of the fiber,  $h$  is the heat transfer coefficient between the fiber and the surrounding medium,  $\eta$  is the fraction of the absorbed pumping power turned to heat, and  $P_P(z)$  is the pumping power distribution along the fiber. It can be understood from (6) that the refractive index of the fiber would change along the fiber depending on the pumping power distribution. If the pumping power has a high power decay rate such that the power is zero at the other end, the refractive index near the pumping port is changed while the refractive index at the other port is kept unchanged. The Bragg wavelength in relation with the refractive index is given by  $\lambda_B = 2n(z)\Lambda$ , where  $n(z)$  is the refractive index along the fiber and  $\Lambda$  is the period of the grating. If the refractive index along the fiber is changed due to the nonuniform distribution of the pumping power, the dispersion profile of the LCFBG is changed. For example, if an LCFBG is pumped from the long-period end, the wavelength of the reflection edge will be shifted to a longer wavelength, and the total reflection bandwidth is increased. On the other hand, if an LCFBG is pumped from the short-period end, the reflection bandwidth is decreased. By considering the relationship between the dispersion and the group-delay slope given by

$$\ddot{\Phi} = \frac{-\lambda_0^2}{c} \times \frac{d\tau}{d\lambda} \quad (7)$$

where  $\lambda_0$  is the central wavelength of the reflection spectrum,  $c$  is the speed of light in vacuum, and  $(d\tau)/(d\lambda)$  is the group-delay slope in the reflection bandwidth, we can see that by increasing the reflection bandwidth, the group-delay slope is reduced, thus leading to a decreased dispersion.

### III. EXPERIMENT AND DISCUSSIONS

The proposed technique based on the setup shown in Fig. 1 is experimentally demonstrated. Two LCFBGs are fabricated and are connected before and after the MZM. In the experiment, since only a 980-nm pump source is available, only an LCFBG written in an Er/Yb co-doped fiber is optically pumped, which is LCFBG2, and LCFBG1 is written in a regular photosensitive fiber and is not pumped. Thus, the frequency tuning is done by pumping LCFBG2 only. A 3-GHz sinusoidal signal generated by the AWG is applied to the MZM via the RF port. The temporally stretched optical pulse from LCFBG1 is then modulated by the 3-GHz sinusoidal microwave signal at the MZM. To avoid dispersion-induced power penalty, the MZM is biased at the minimum transmission point. The modulated signal is then sent to LCFBG2, and the reflected optical signal

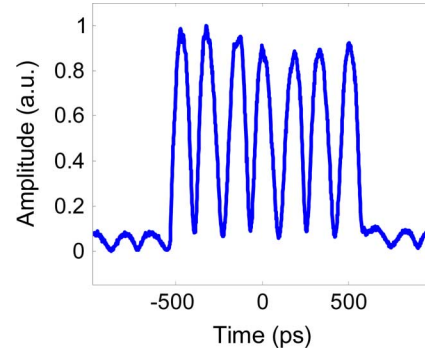


Fig. 2. Modulated signal at the output of the MZM observed by the sampling oscilloscope.

is detected by a high-speed PD, with the electrical waveform monitored by a sampling oscilloscope. Note that the MLL, the AWG, and the sampling oscilloscope are synchronized. The bandwidth of LCFBG1 is 0.8 nm and its value of dispersion is  $\ddot{\Phi}_1 = 11.5 \times 10^3 \text{ ps}^2$ . The bandwidth of LCFBG2 is 0.5 nm and its value of dispersion is  $\ddot{\Phi}_2 = 12 \times 10^3 \text{ ps}^2$  if it is pumped.

An ultrashort Gaussian pulse with a full-width at half-maximum bandwidth of 8 nm, centered at 1558 nm is generated by the MLL and is sent to LCFBG1 via the first optical circulator. After reflecting from LCFBG1, the optical pulse is temporally stretched and the time duration of the pulse is increased to  $\Delta t = \Delta f \times \ddot{\Phi}_1 = 1150 \text{ ps}$ , where  $\Delta f$  is the 3 dB bandwidth of LCFBG2 which is 0.8 nm or equivalently 100 GHz. The temporally stretched pulse is modulated at the MZM by the 3-GHz microwave drive signal. Since the MZM is biased at the minimum transmission point, the output signal from the MZM is frequency doubled. Considering the duration of the input optical pulse to the MZM is 1150 ps and the frequency doubling operation at the MZM, the signal at the output of the MZM should contain seven microwave cycles. Fig. 2 shows the experimentally generated signal with photodetection from the output of the MZM, observed by the sampling oscilloscope. As can be seen, the time duration of the modulated signal is 1150 ps and the number of microwave cycles is 7.

The optical pulse at the output of the MZM is then sent to LCFBG2 via the second optical circulator. LCFBG2 is written in an Er/Yb co-doped fiber and is pumped by a 980-nm LD from the long-period end. As discussed in Section II, by pumping an LCFBG from the long-period end, the wavelength at the spectrum edge will be shifted to a longer wavelength. As a result, the group-delay slope in the reflection band is decreased and the dispersion is decreased consequently. Fig. 3(a) and (b) shows the reflection spectra and the group delay responses of the LCFBG2 pumped by the 980-nm LD at different pumping powers. Since LCFBG2 is pumped from the long-period end, by increasing the pump power, the reflection bandwidth is increased, the group-delay slope is decreased, and thus based on (7) the dispersion is decreased. On the other hand, if LCFBG2 is pumped from the short-period end, the dispersion would be increased by increasing the pumping power. Therefore, by continuously tuning the pumping power to change the dispersion of LCFBG2, the frequency multiplication factor would be changed continuously. In the experiment, since

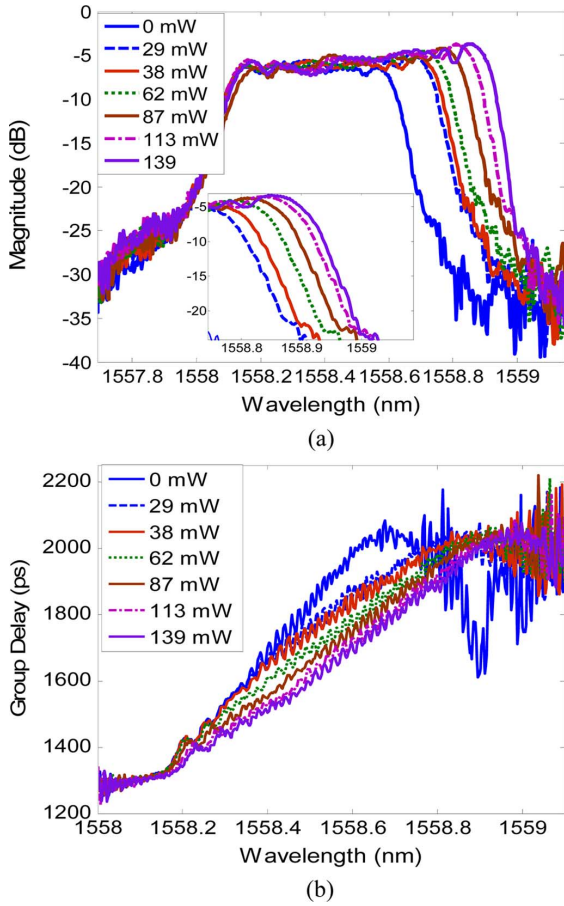


Fig. 3. (a) Magnitude and (b) group delay responses of the Er/Yb co-doped LCFBG pumped with a 980-nm LD at different power levels. The inset in (a) gives a zoom-in view of the magnitude response near the long reflection edge.

the dispersion of LCFBG1 is constant, and the dispersion of LCFBG2 is increased, the multiplication factor  $F$  is decreased. In the demonstration, the pumping power is increased from 29 to 139 mW, and the dispersion of the LCFBG2 is reduced from 9704 to 7583.74 ps<sup>2</sup>, as shown in Fig. 3(b). Based on (5), the multiplication factor is, thus, reduced from 12.8 to 5.88. Note that the bandwidth of LCFBG2 is changed when it is pumped, as can be seen from Fig. 3(a), where the bandwidth is increased from 0.5 to 0.78 nm when the pumping power is increased from 0 to 139 mW. The number of microwave cycles within the pulse is determined by the overall bandwidths of LCFBG1 and LCFBG2. If the overall bandwidth is 0.5 nm, the number of cycles in the modulated signal would be 5. Note that the bandwidth of LCFBG1 is 0.8 nm and the effective bandwidth of LCFBG2 is increased if pumped, the number of cycles in the modulated signal will also be increased.

Fig. 4 shows the experimentally generated microwave waveforms by pumping LCFBG2 at different pumping power levels. In the experiment, the pumping power is increased from 29 to 139 mW (the injection current to the LD is increased from 50 to 180 mA), the microwave frequency is reduced from 35.71 to 15.34 GHz, and the multiplication factor  $F$  is reduced from 11.9 to 5.14. Note that the number of microwave cycles in the pulse is increased because of the increase of the bandwidth of LCFBG2 when it is pumped.

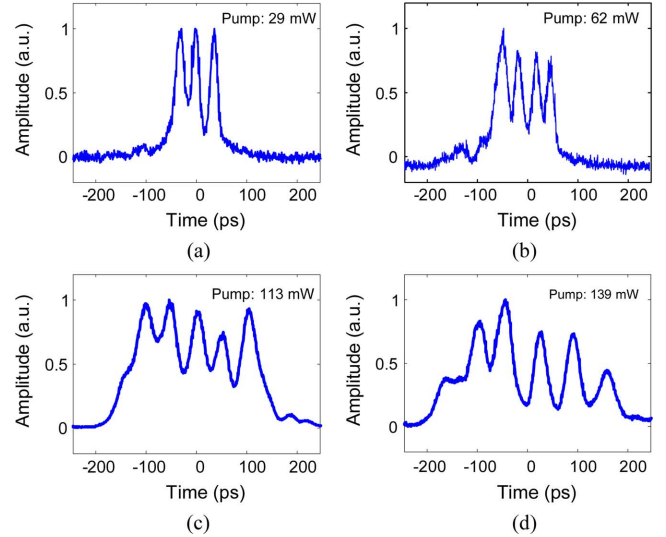


Fig. 4. Generated microwave waveforms when LCFBG2 is pumped with pumping powers of 29, 62, 113, and 139 mW and corresponding frequencies of (a) 35.71, (b) 28.57, (c) 19.23, and (d) 15.43 GHz.

To avoid the change of the pulse width, we stretch LCFBG2 to make its long reflection edge aligned with the long reflection edge of LCFBG1. Then, when it is pumped, the overall bandwidth is fixed at 0.5 nm with no change. The generated microwave waveforms are shown in Fig. 5. By increasing the pumping power from 38 to 139 mW (the injection current to the LD is increased from 60 to 180 mA), the microwave frequency is decreased from 35 to 15.38 GHz, and the multiplication factor  $F$  is reduced from 11.66 to 5.13. A summary is provided in Table I, with both the theoretical and experimental values provided.

The frequency tunable range in the proposed system depends on the values of dispersion of LCFBG1 and LCFBG2, which can be increased if four pumping LDs are employed. In this case, two pumping LDs are employed to pump one LCFBG from the two ends. For example, if the values of dispersion and the bandwidths of LCFBG1 and LCFBG2 are 13200 and 10560 ps<sup>2</sup>, and 0.5 and 0.65 nm, respectively, and if LCFBG2 is pumped from the two ends, its value of dispersion can be tuned from 8075.28 to 13728 ps<sup>2</sup>, and consequently, the multiplication factor can be tuned continuously from 5 to 44.

To evaluate how the generated waveforms are close to the theoretical waveforms given by (4), a simulation is performed to compare the simulated waveforms with the waveforms generated in the experiment. Fig. 6 shows the simulated and experimentally generated microwave waveforms for LCFBG2 being pumped at two power levels of 62 and 87 mW. In the simulation, the reflection spectra of the two LCFBGs are the actual spectra of the LCFBGs used in the experiment. As can be seen, the simulated and the experimentally generated waveforms match quite well. The small discrepancy between the simulated and the experimentally generated waveforms is mainly resulted from the limited bandwidths of the MZM and the PD.

The key components in the proposed system for microwave waveform generation are the two LCFBGs. An ideal LCFBG would exhibit a constant magnitude response and a linear group

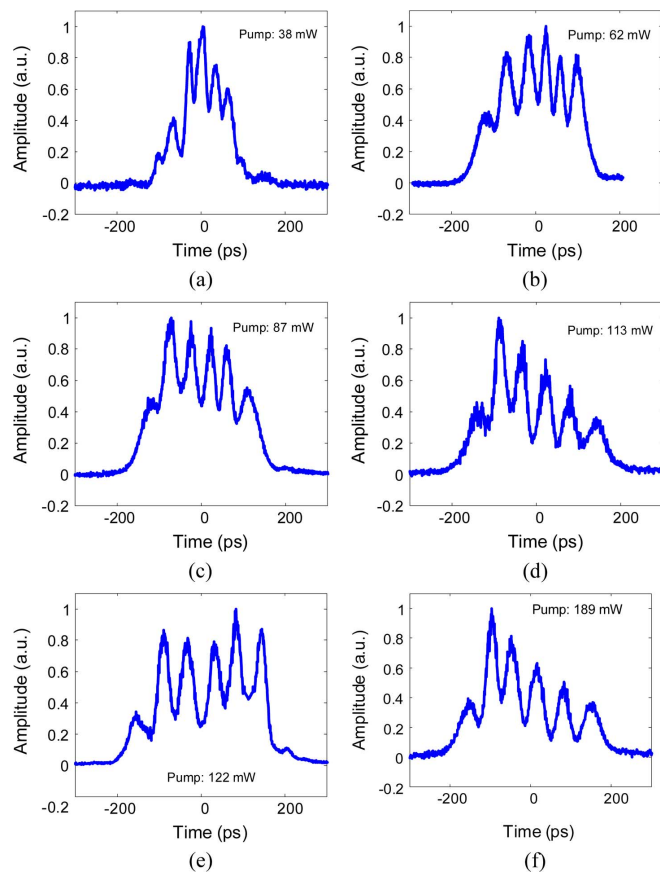


Fig. 5. Generated microwave waveforms when LCFBG2 is pumped with pumping powers of 38, 62, 87, 113, 122, and 139 mW, and corresponding frequencies of (a) 35, (b) 27.27, (c) 22.22, (d) 18.51, (e) 17.24, and (f) 15.38 GHz.

TABLE I  
SUMMARY OF THE KEY PARAMETERS FOR THE THEORETICAL WAVEFORMS AND THE WAVEFORMS GENERATED EXPERIMENTALLY

Pumping power/Injection current	$\Phi_2$ (ps <sup>2</sup> )	$F$ Experimental/ Theoretical	$f_{RF}$ (GHz) Experimental / Theoretical
29 mW/50 mA	9614.00	11.90/12.20	35.71/36.6
38 mW/60 mA	9548.38	11.66/11.78	35.00/35.34
62 mW/90 mA	9032.18	9.06/9.32	27.27/27.96
87 mW/120 mA	8579.71	7.40/7.78	22.22/23.34
113 mW/150 mA	7950.61	6.17/6.48	18.51/19.44
139 mW/180 mA	7392.85	5.13/5.60	15.38/16.80

delay response with no ripples. In a practical LCFBG, however, ripples in the magnitude and group delay responses would always exist, which may affect the performance for microwave waveform generation. To evaluate the impact due to the magnitude and group delay ripples on the generated waveforms, a second simulation is performed. Since the period of the ripples depends on the phase mask used for writing the LCFBGs, for a specific phase mask, the period of the ripples is constant, but the amplitudes of the magnitude and group delay ripples

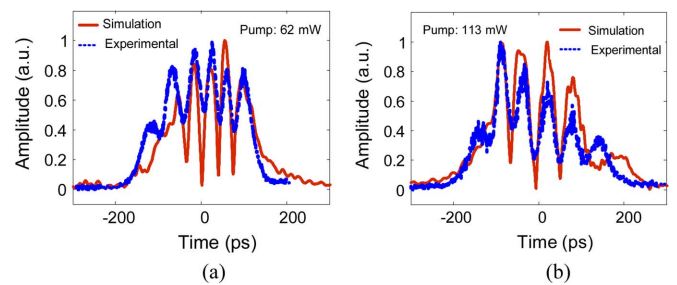


Fig. 6. Comparison of the waveforms generated experimentally and the waveforms obtained based on simulation for LCFBG2 being pumped at (a) 62 and (b) 113 mW.

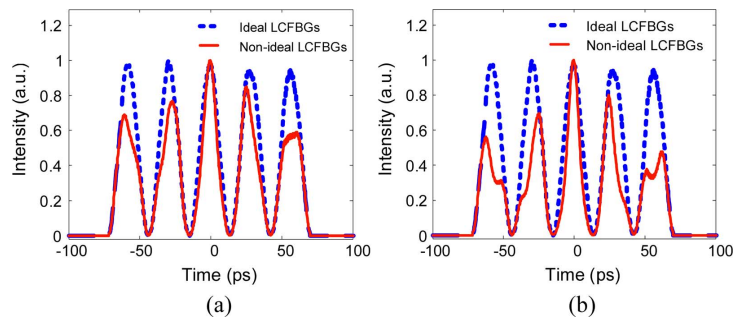


Fig. 7. Simulation of the generated microwave waveforms for the LCFBGs with magnitude ripples only. The period of the magnitude ripples is set at 60 pm and the amplitude of the ripples is set at two values of (a) 0.4 dB and (b) 0.8 dB.

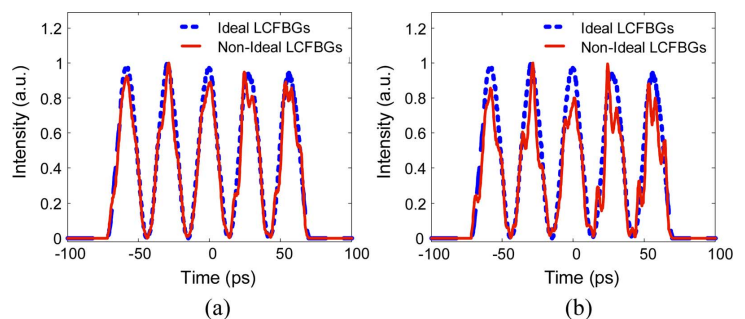


Fig. 8. Simulation of the generated microwave waveforms for the LCFBGs with group delay ripples only. The period of the group delay ripples is set to 20 pm and the amplitude of the ripples is set at two values of (a) 30 ps and (b) 60 ps.

may change depending on the writing technique. A usual way to reduce the ripples is to apply apodization and back scanning during the fabrication process. In this simulation, the period of the ripples is considered constant and the amplitudes of the magnitude and group delay ripples are set at different values.

First, we assume that the LCFBGs have an ideal group delay response and the ripples only exist in the magnitude response. Fig. 7(a) and (b) shows the simulated waveforms for the magnitude ripples having a period of 60 pm and an amplitude at two values of 0.4 and 0.8 dB, respectively. As can be seen, the magnitude ripples of the LCFBGs would cause distortions to the generated waveforms, and the distortions are increased when the amplitude of the magnitude ripples is increased.

Then, the impact of group delay ripples on the generated waveforms is studied. In the simulation, a constant magnitude response is considered. Again, the period of the ripples is set

at a fixed value, which is 20 pm. Fig. 8(a) and (b) shows waveforms for the group delay ripples with an amplitude of 30 and 60 ps, respectively. As can be seen, the group delay ripples would also cause distortions to the generated waveforms, and the distortions become stronger when the amplitude of the ripples is increased. In reality, we have both ripples in the magnitude and group delay (Kramer–Kronig relations) which makes the situation worse. To reduce both the magnitude and group delay ripples, we may apply apodization during the fabrication of the LCFBGs.

#### IV. CONCLUSION

A novel method for achieving tunable microwave frequency multiplication based on an unbalanced TPS system using two LCFBGs written in Er/Yb co-doped fibers was proposed and demonstrated. The key significance of the proposed technique is the tuning of the frequency multiplication factor through optical pumping of the LCFBGs. A theoretical analysis was provided which was verified by an experiment. Microwave waveform generation with a tunable frequency multiplication factor from 5.13 to 11.9 was experimentally demonstrated. The impact of the ripples of the LCFBGs on the performance of the system was also studied. The results showed that both the magnitude and group delay ripples would lead to distortions to the generated waveforms. A solution to reduce the ripples is to apply apodization in the fabrication of the LCFBGs. The proposed technique has potential applications in radar, communications, and microwave tomography where high frequency and frequency-tunable microwave waveforms are needed.

#### REFERENCES

- [1] J. D. McKinney, D. S. Seo, D. E. Leaird, and A. M. Weiner, "Photonically assisted generation of arbitrary millimeter-wave and microwave electromagnetic waveforms via direct space-to-time optical pulse shaping," *J. Lightw. Technol.*, vol. 21, no. 12, pp. 3020–3028, Dec. 2003.
- [2] C. Wang and J. P. Yao, "Photonic generation of chirped millimeterwave pulses based on nonlinear frequency-to-time mapping in a nonlinearly chirped fiber Bragg grating," *IEEE Trans. Microw. Theory Tech.*, vol. 56, no. 2, pp. 542–553, Feb. 2008.
- [3] M. Bertero, M. Miyakawa, P. Boccacci, F. Conte, K. Orikasa, and M. Furutani, "Image restoration in chirp pulse microwave CT (CP-MCT)," *IEEE Trans. Biomed. Eng.*, vol. 47, no. 5, pp. 690–699, May 2000.
- [4] J. U. Kang, M. Y. Frankel, and R. D. Esman, "Demonstration of microwave frequency shifting by use of a highly chirped mode-locked fiber laser," *Opt. Lett.*, vol. 23, no. 15, pp. 1188–1190, Aug. 1998.
- [5] J. M. Fuster, D. Novak, A. Nirmalathas, and J. Marti, "Single-sideband modulation in photonic time-stretch analogue-to-digital conversion," *Electron. Lett.*, vol. 37, no. 1, pp. 67–68, Jan. 2001.
- [6] J. Azana, N. K. Berger, B. Levit, V. Smulakovsky, and B. Fischer, "Frequency shifting of microwave signals by use of a general temporal self-imaging (Talbot) effect in optical fibers," *Opt. Lett.*, vol. 29, no. 24, pp. 2849–2851, Dec. 2004.
- [7] C. Wang, M. Li, and J. P. Yao, "Continuously tunable photonic microwave frequency multiplication by use of an unbalanced temporal pulse shaping system," *IEEE Photon. Technol. Lett.*, vol. 22, no. 17, pp. 1285–1287, Sep. 2010.

- [8] H. Shahoei, M. Li, and J. Yao, "Continuously tunable time delay using an optically pumped linear chirped fiber Bragg grating," *J. Lightw. Technol.*, vol. 29, no. 10, pp. 1465–1472, May 2011.
- [9] M. Li and J. P. Yao, "Photonic generation of continuously tunable chirped microwave waveforms based on a temporal interferometer incorporating an optically-pumped linearly-chirped fiber Bragg grating," *IEEE Trans. Microw. Theory Tech.*, vol. 59, no. 12, pp. 3531–3537, Dec. 2011.
- [10] M. A. Muriel, J. Azana, and A. Carballar, "Real-time Fourier transformer based on fiber gratings," *Opt. Lett.*, vol. 24, no. 1, pp. 1–3, Jan. 1999.
- [11] Y. Han, Z. Li, S. Pan, M. Li, and J. P. Yao, "Photonic-assisted tunable microwave pulse fractional Hilbert transformer based on temporal pulse shaping system," *IEEE Photon. Technol. Lett.*, vol. 23, no. 9, pp. 570–572, May 2011.
- [12] H. Chi and J. P. Yao, "Symmetrical waveform generation based on temporal pulse shaping using amplitude-only modulator," *Electron. Lett.*, vol. 43, no. 7, pp. 415–417, Mar. 2007.

**Hiva Shahoei** (S'09) received the B.Sc. degree in electrical engineering from Tabriz University, Tabriz, Iran, in 2005, and the M.Sc. degree in electrical engineering from Tehran Polytechnic University, Tehran, Iran, in 2008. She is currently working toward the Ph.D. degree in electrical and computer engineering in the Microwave Photonics Research Laboratory, School of Electrical Engineering and Computer Science, University of Ottawa, Ottawa, ON, Canada.

Her current research interests include fiber Bragg grating and its applications to microwave photonics, slow/fast light and its applications in microwave photonics, and ultrafast optical signal processing.

**Jianping Yao** (M'99–SM'01–F'12) received the Ph.D. degree in electrical engineering from the Université de Toulon, Toulon, France, in December 1997.

He joined the School of Electrical Engineering and Computer Science, University of Ottawa, Ottawa, ON, Canada, as an Assistant Professor in 2001, where he became an Associate Professor in 2003, a Full Professor in 2006, and the University Research Chair in 2007. From July 2007 to June 2010, he was the Director of the Ottawa-Carleton Institute for Electrical and Computer Engineering. Prior to joining the University of Ottawa, he was an Assistant Professor in the School of Electrical and Electronic Engineering, Nanyang Technological University, Singapore, from 1999 to 2011. He is a principal investigator of more than 20 projects, including five strategic grant projects funded by the Natural Sciences and Engineering Research Council of Canada. He has published more than 360 papers, including more than 200 papers in peer-reviewed journals and 160 papers in conference proceedings. His research interests focus on microwave photonics, which includes photonic processing of microwave signals, photonic generation of microwave, millimeter-wave and terahertz, radio over fiber, ultrawideband over fiber, and photonic generation of microwave arbitrary waveforms. His research also covers fiber optics and biophotonics, which includes fiber lasers, fiber and waveguide Bragg gratings, fiber-optic sensors, microfluidics, optical coherence tomography, and Fourier-transform spectroscopy.

Dr. Yao is currently an Associate Editor of the *International Journal of Microwave and Optical Technology*. He is on the Editorial Board of the IEEE TRANSACTIONS ON MICROWAVE THEORY AND TECHNIQUES. He is the Chair of numerous international conferences, symposia, and workshops, including the Vice Technical Program Committee (TPC) Chair of the IEEE Microwave Photonics Conference in 2007, the TPC Co-Chair of the Asia-Pacific Microwave Photonics Conference in 2009 and 2010, the TPC Chair of the high-speed and broadband wireless technologies subcommittee of the IEEE Radio Wireless Symposium in 2009–2012, the TPC Chair of the microwave photonics subcommittee of the IEEE Photonics Society Annual Meeting in 2009, the TPC Chair of the IEEE Microwave Photonics Conference in 2010, and the General Co-Chair of the IEEE Microwave Photonics Conference in 2011. He is also a committee member of numerous international conferences. He also received the 2005 International Creative Research Award at the University of Ottawa. He was the recipient of the 2007 George S. Glinski Award for Excellence in Research and the Natural Sciences and Engineering Research Council of Canada Discovery Accelerator Supplements Award in 2008. He is a registered Professional Engineer of Ontario. He is a Fellow of the Optical Society of America, and a Fellow of the IEEE Microwave Theory and Techniques Society and the IEEE Photonics Society.